

Searching for twins of the V1309 Sco progenitor system: a selection of long-period contact binaries

Alexander Kurtenkov^{1,2}

¹ Department of Astronomy, University of Sofia, 5 James Bourchier Blvd., 1164 Sofia, Bulgaria

² Institute of Astronomy and National Astronomical Observatory, Bulgarian Academy of Sciences, 72 Tsarigradsko Shose Blvd., 1784 Sofia, Bulgaria
al.kurtenkov@gmail.com

(Submitted on xx.xx.xxxx; Accepted on xx.xx.xxxx)

Abstract. The only well-studied red nova progenitor (V1309 Sco) was a contact binary with a 1.4-day period. The prospects for searching for similar systems, as well as stellar merger candidates in general, are explored in this work. The photospheric temperatures of 128 variables with periods $P = 1.1 - 1.8$ d classified as W UMa-type binaries are calculated using their colors listed in the SDSS catalog. A selection of 15 contact binaries with similar temperatures and periods as the V1309 Sco progenitor is thus compiled. The Kepler Eclipsing Binary Catalog is used to analyse systems with eclipse timing variations (ETV) possibly caused by changes of the orbital period. Out of the 31 systems with parabolic ETV curves listed by Conroy et al. (2014, AJ, 147, 45) two could be contact binaries with a decreasing period and, therefore, potential stellar merger candidates. Out of the 569 contact binaries in the OGLE field analysed by Kubiak et al. (2006, AcA, 56, 253) 14 systems have periods longer than 0.8 d and a statistically significant period decrease.

Key words: Stars: binaries: eclipsing – Stars: individual: V1309 Sco – Stars: evolution

1. Introduction

The outburst of V1309 Sco in 2008 has played a key role in our understanding of the rare red nova eruptions. Very few such events were previously known. The well-studied V838 Mon (Bond et al. 2003) had shown distinct similarities in its spectral evolution to transients V4332 Sgr and M31 RV. Tytenda & Soker (2006) suggested that all three events were caused by mergers in binary stars. However, it was not until the eruption of V1309 Sco that direct observations of a red nova progenitor could support this theory.

Mason et al. (2010) presented thorough observations of the V1309 Sco outburst and pointed out its similarities to red novae. They derived a peak absolute magnitude of $M_V = -8.3$ mag and a maximum emission line FWHM of ~ 150 km/s. Tytenda et al. (2011) used archive data from the OGLE project to show that the progenitor is a W UMa (contact) binary with a period of 1.44 d and a ~ 0.2 mag amplitude. Moreover, the period had been decreasing exponentially for at least six years before the outburst, reaching 1.42 d in 2007. The OGLE lightcurve also showed slow brightness variations as the I magnitude remained in the range 16 – 17 mag before the outburst. Tytenda et al. (2011) obtained an effective temperature of the progenitor of 4500 K under certain approximations for the interstellar reddening. An exact value was difficult to derive due to the proximity of V1309 Sco to the galactic plane.

Five galactic red novae are currently known – V4332 Sgr, V838 Mon, V1309 Sco, the highly reddened OGLE-2002-BLG-360 and allegedly, the 1670 eruption of CK Vul (Kaminski et al. 2015). With the addition of several extragalactic transients, such as M31 RV (Rich et al. 1989), M85 OT2006-1 (Kulkarni et al. 2007), and M31LRN 2015 (Kurtenkov et al. 2015), they constitute a rare class of mostly very luminous events. As of 2016 V1309 Sco remains the only red nova with a well-studied progenitor, and the only direct proof that stellar mergers cause red novae.

2. Motivation

The archival observations of V1309 Sco have presented the unique opportunity of studying the transition of a stellar merger process from a quiescent phase (eclipsing binary with a decreasing orbital period) to a dynamic phase (red nova explosion, ultimately leaving the merger product engulfed in dust). A prediction of such an event will allow for a much more detailed exploration of the progenitor system, e.g. mass and temperature determination via multicolor photometry, or observing the spectral evolution of the common envelope. Such results can be used to improve the relations between the parameters of the progenitor system and the parameters of the transient. An attempt at studying these relations was made by Kochanek et al. (2014), although the statistical sample is still quite small. A red nova prediction was made by Molnar et al. (2015) for the Kepler eclipsing binary KIC 9832227.

As discussed by Tytenda et al. (2011) the merging can be triggered by the evolution of the primary component. It grows in size as it crosses the Hertzsprung gap and the system starts losing mass and

angular momentum through the L_2 Lagrangian point. As the V1309 Sco progenitor probably included an evolved K-star, this scenario is compatible with the observations. Furthermore, the observed orbital period of 1.44 d is unusually long for W UMa-type binaries, so it requires a large semi-major axis, and respectively, large radii. Similarly, many long-period contact binaries can be seen as potential merger candidates and their exploration could give us an insight into the physics of red nova progenitors.

The last decades have shown a radical increase in the number of known eclipsing binary systems, owing to modern time-based sky surveys, such as NSVS, ASAS, and most recently, the Catalina Sky Survey. The latter has produced a catalog including ~ 31000 contact and ellipsoidal binaries (Drake et al. 2014). As of June 2016 the VSX (Variable Star Index) database lists a total of 39634 W UMa-type binaries. The present work aims to show that the number of known contact binaries is sufficient to draw an object selection of possible V1309 Sco-like systems. Contact binaries that show similar characteristics as V1309 Sco could be at the same evolutionary stage at which the mechanism that led to the 2008 eruption is triggered. The selected systems in Section 3 could prove to be promising targets of follow-up observations, aiming to derive their absolute parameters and to look for period changes.

Another important addition to the exploration of eclipsing binaries has been the Kepler Eclipsing Binary Catalog (Slawson et al. 2011). It could be a powerful tool in the search of stellar merger candidates as it provides high-quality lightcurves with exact minima timing. Section 4 is dedicated to selecting stellar merger candidates from Kepler and OGLE binaries with considerable eclipse timing variations.

3. SDSS/VSX color-based selection

Binaries of the W UMa type have typical orbital periods in the range 0.2 – 0.8 d. However, the VSX database currently lists 1125 W UMa binaries with $P > 1$ d. Some of them are misclassified β Lyrae as those variables have similar lightcurve shapes but generally larger periods. The distribution of cataloged long-period W UMa binaries is shown in Fig. 1. In the 1.0 – 2.0 d period range there are still relatively many systems cataloged as W UMa binaries. Also plotted is how the ratio of cataloged W UMa to β Lyr binaries changes with the orbital period. In case all systems in the 1.0 – 2.0 d period range cataloged as contact binaries were misclassified β Lyrae, this ratio would not decrease after $P \sim 2.0$ d. Many systems in this period range could be contact binaries with one or two evolved components and, therefore, objects of the current study.

The somewhat narrower period range between 1.1 d and 1.8 d is approximately centered on the V1309 Sco period. As of June 2016 the VSX lists 506 systems of the W UMa type in it. Of those, 207 were identified in the ninth release of the SDSS catalog (Ahn et al. 2012) within a search radius of $2''$. The SDSS catalog provides multicolor photometry in the Sloan *ugriz* passbands. The imaging data of a given object is obtained with a 72 sec delay between two consecutive filters, so there is a ~ 5 min interval between the *r*-band and *g*-band frames. Therefore it can be safely assumed that the imaging of $P > 1$ d binaries in all passbands is simultaneous. The colors of contact binaries slightly vary with phase due to the temperature difference of the components and the gravity darkening effect. Both effects are of the order of $\sim 10^2$ K, which allows for a satisfactory estimate of the temperature of the common envelope using multicolor photometry at a given phase. The color-temperature relations derived by Boyajian et al. (2013) were used for this purpose. These relations are of the form

$$T_{eff} = a_0 + a_1 X + a_2 X^2 + a_3 X^3, \quad (1)$$

where X represents the color index and T_{eff} is the effective photospheric temperature. The coefficients derived by Boyajian et al. (2013) for the Sloan photometric system are given in Tab. 1.

Table 1. Polynomial coefficients of the color-temperature relation extracted from Boyajian et al. (2013).

Color index	a_0	a_1	a_2	a_3	Range [mag]
g-r	7526	-5570	3750	-1332.9	-0.23 – 1.40
g-i	7279	-3356	1112	-153.9	-0.43 – 2.78
g-z	7089	-2760	804	-95.2	-0.58 – 3.44

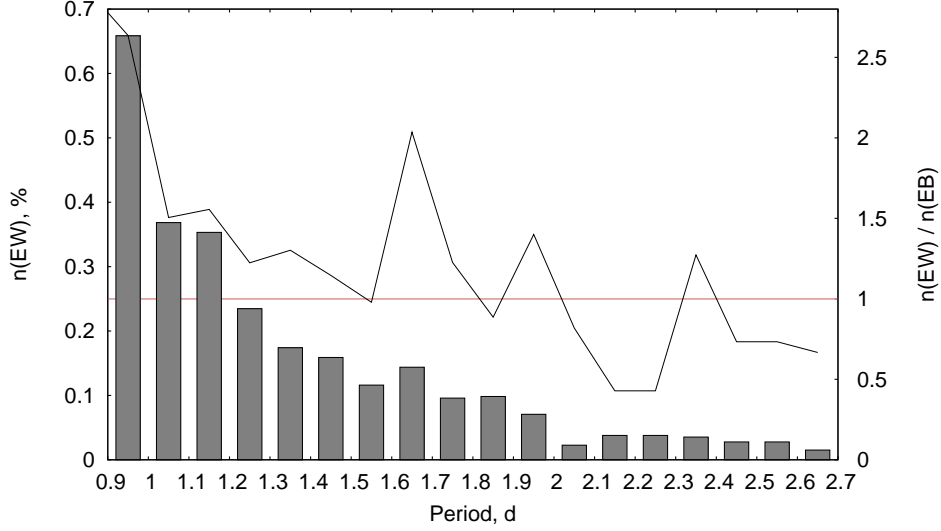


Fig. 1. The bars represent the period distribution of systems classified as W UMa binaries for $P > 0.9$ d, expressed in percentages of all 39634 such systems in the VSX. The dark line represents the ratio of cataloged W UMa to β Lyr binaries for each period interval. The ratio decreases after $P \sim 2.0$ d, which implies that the majority of cataloged W UMa binaries with periods in the $1.0 - 2.0$ d range are not misclassified β Lyrae. The left y-scale applies to bars, while the right y-scale applies to lines. All data is extracted from the VSX database.

Table 2. A selection of 23 contact binaries with $P = 1.1 - 1.8$ d and $T_{eff} = 4200 - 4800$ K. The temperatures of the systems correspond to spectral types K0III-K3III and are similar to the V1309 Sco progenitor. The last column contains the values of the total galactic reddening along the line-of-sight (the maximum possible reddening of the object). The visual (wide band V) magnitudes and amplitudes are extracted from the VSX database.

α (J2000.0)	δ (J2000.0)	P [d]	Mag.	Amp.	SDSS epoch	T_{eff} [K]	σ_T [K]	$E(B - V)_0$
10:00:01.70	24:23:05.1	1.2955	15.85	0.15	2004.9566	4213	48	0.03
13:06:00.14	18:00:46.7	1.3074	16.68	0.14	2005.4271	4315	70	0.02
05:44:53.66	03:18:35.0	1.1997	16.17	0.18	2007.8835	4365	100	0.75
16:56:09.74	42:42:19.7	1.2699	15.52	0.18	2004.4527	4383	127	0.02
03:29:54.17	38:01:44.9	1.3618	14.22	0.25	2003.0859	4398	66	0.27
08:31:48.57	29:44:44.0	1.4136	14.93	0.12	2002.9988	4445	89	0.03
05:44:07.39	28:31:40.8	1.2753	15.77	0.78	2003.9705	4456	130	1.26
17:14:28.01	10:13:10.7	1.7623	15.92	0.14	2005.4380	4479	61	0.10
02:09:03.05	-04:26:14.7	1.5781	18.17	0.31	2005.7421	4496	116	0.02
08:17:46.29	13:05:05.7	1.5947	14.90	0.08	2004.9704	4519	64	0.02
07:34:32.94	36:48:28.5	1.1646	17.38	0.31	2000.2604	4519	96	0.05
05:07:27.74	16:13:10.5	1.1861	15.21	0.23	2006.8322	4528	60	0.31
22:29:09.15	17:37:23.4	1.3664	14.60	0.08	2009.7912	4568	46	0.06
14:21:14.77	35:28:38.9	1.5851	16.14	0.09	2003.3164	4592	26	0.02
04:25:51.08	30:02:48.9	1.1489	15.72	0.38	2002.9984	4613	100	0.39
04:39:40.76	19:18:53.3	1.7422	13.92	0.30	2006.0841	4658	99	0.34
23:15:47.32	12:29:37.5	1.7325	15.28	0.19	2008.8385	4679	75	0.06
04:45:50.71	11:34:57.2	1.3164	15.29	0.35	2006.8321	4723	110	0.51
15:02:20.15	26:21:12.1	1.7954	15.94	0.18	2004.3649	4729	83	0.04
07:26:18.08	31:55:03.0	1.1579	15.71	0.22	2006.8870	4744	67	0.06
09:46:14.73	16:47:06.0	1.6007	15.31	0.25	2005.1943	4750	100	0.03
00:44:12.88	20:11:07.8	1.7533	13.75	0.06	2009.0463	4750	77	0.04
10:02:30.35	50:18:08.8	1.2404	15.51	0.23	2001.8904	4760	74	0.01

Three color temperatures (T_{g-r} , T_{g-i} and T_{g-z}) were calculated for each of the 207 objects. The photospheric temperature T_{eff} and its statistical standard error σ_T were then calculated as an average of the three values and the RMS of the residuals, respectively. Photospheric temperatures for 143 systems were thus obtained. The color indices of 9 objects are outside the calibration range. The remaining 55 objects (26 % of all) have $\sigma_T > 150$ K and were excluded from the sample. The results are in the range 3230 – 7560 K (median temperature 5150 K), with a median error $\sigma_T = 80$ K.

The 23 systems with $T_{eff} = 4200 - 4800$ K are listed in Tab. 2. Giants of the K0III-K3III types have effective temperatures in this range. It should be noted that the interstellar reddening has been neglected for this calculation, so it is plausible only for objects that are far from the galactic plane, where the reddening is weak. For 15 of the 23 systems the total galactic reddening along the line-of-sight is less than 0.07 mag. If these are correctly classified as W UMa binaries, they may have similar parameters to the V1309 Sco progenitor. Follow-up observations of these systems are therefore encouraged.

Of the 143 systems 128 have galactic latitudes $|b| > 20^\circ$, which implies a low reddening. The calculated photospheric temperatures for all 128 systems are presented in the online Tab. 5.

4. Kepler and OGLE candidates

The objects selected in Section 3 might be of a similar evolutionary stage as the progenitor of V1309 Sco, but it is highly improbable that they will erupt in the upcoming decades. The best way to predict such an event is based on minima timing as the decrease of the orbital period before merging causes eclipse timing variations (ETV). The most reliable source of such information is by far the Kepler mission.

Table 3. Kepler systems classified after visual inspection. The following designations are used: EA = Algol, EB = β Lyr, EW = W UMa, ELV = ellipsoidal variable; Pos = positive, Neg = negative.

KIC	P [d]	type	$d^2 ETV/dt^2$	KIC	P [d]	type	$d^2 ETV/dt^2$
2305372	1.404	EA	Pos	6677225	0.525	ELV/EW	Pos
3104113	0.846	EW	Pos	7696778	0.331	EW	Pos
3765708	0.431	ELV/EW	Pos	7938468	7.226	EA	Pos
4074532	0.353	EW	Pos	7938870	0.580	EA/EB	Neg
4851217	2.470	EA	Pos	8758161	0.998	EA	periodic?
4853067	1.340	ELV/EB	Neg	9087918	0.445	EW	Pos
5020034	2.119	EA	Pos	9402652	1.073	EA	periodic?
5471619	0.962	EA/EB	Neg	9840412	0.878	EW	Neg
5770860	0.737	ELV/EW	Pos	9934052	0.352	ELV/EW	Pos
5792093	0.600	EB	Neg	10030943	0.235	ELV/EW	Pos
6044064	5.063	EA	Pos	10292413	0.559	ELV/EW	Neg
6044543	0.532	EB	Neg	10736223	1.105	EA	Pos
6066379	1.303	EA	Neg	11097678	0.999	EW	Pos
6213131	0.561	EB	Pos	11144556	0.642	EW	Pos
6314173	1.433	EA	Neg	11924311	0.445	EB/EW	Pos
6464285	0.843	EA	Pos

The presence of ETV does not necessarily imply a loss of angular momentum from the system. It is far more likely to be caused by mass transfer between the components or by signal delay due to perturbations by a third body (light travel time effect, LTTE). In the latter case the ETV curve exhibits strict periodicity. In the former case, which is quite common for β Lyrae, the second derivative of the ETV curve can be positive as well as negative. Only contact binaries with parabolic ETV curves with a negative second derivative could undergo a stellar merger in the near future.

The ETV signals of 1279 Kepler binaries were analysed by Conroy et al. (2014). The authors found 31 systems with nearly parabolic ETV curves over the whole ~ 1400 d period of observation. The type of variability was determined for all 31 systems after visual inspection of the lightcurves and ETV curves (Tab. 3). Just two contact binaries with a negative second derivative of the ETV curve were found:

- KIC 9840412 ($BJD_0 = 2454954.556807$, $P = 0.87845(58 \pm 9)$ d)
- KIC 10292413 ($BJD_0 = 2454954.202209$, $P = 0.55915(88 \pm 4)$ d).

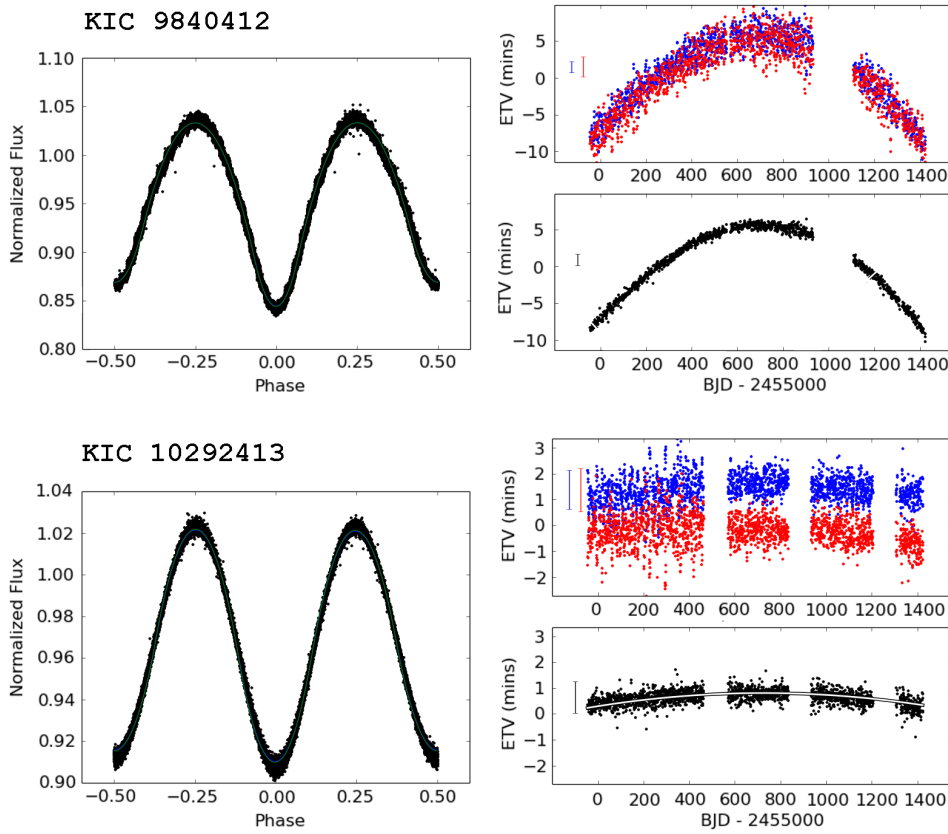


Fig. 2. Lightcurves (*left*) and ETV curves (*right*) of the two selected W UMa binaries in the Kepler field. Both ETV curves (*top*: of both the primary and secondary minima, *bottom*: averaged) have a negative second derivative. The images are retrieved from the Kepler Eclipsing Binaries database at <http://keplerebs.villanova.edu/>.

The latter could as well be an ellipsoidal variable. Note that ellipsoidal variables are hard to distinguish from contact binaries with nearly sinusoidal lightcurves. The lightcurves and ETV curves of the two systems are presented in Fig. 2. The period derivatives were calculated from $\frac{dP}{dt} = P \frac{d^2 ETV}{dt^2}$. The parabolic fits of the ETV curves yielded $dP/dt = -1.196 \pm 0.003 \times 10^{-5}$ d/yr for KIC 9840412 and $-2.737 \pm 0.089 \times 10^{-7}$ d/yr for KIC 10292413. Follow-up observations of these two systems (especially minima timing) are recommended in order to confirm or rule out LTTE as the cause for ETV and to establish whether they can be considered as stellar merger candidates.

The Optical Gravitational Lensing Experiment (OGLE) has also been a reliable source for long-term studies of eclipsing binaries. The period changes of 569 OGLE contact binaries were analysed by Kubiak et al. (2006). Notably, the two systems with the most rapid period decrease have very long periods: 1.36 d and 1.70 d respectively. The error of calculation of period changes is assessed at 2.3×10^{-7} d/yr by the authors. All 14 systems with $P > 0.8$ d and $dP/dt < -2.3 \times 10^{-7}$ d/yr are listed in Tab. 4. They require a large-sized telescope for follow-up observations considering that they are faint objects in a crowded field near the galactic center.

5. Summary and discussion

The only red nova with a well-studied progenitor is V1309 Sco, which erupted in 2008. Its progenitor was a contact binary with an exceptionally long period of ~ 1.44 d, which could be explained by the

Table 4. A selection of long-period OGLE contact binaries with decreasing periods (Kubiak et al. 2006).

α (J2000)	δ (J2000)	I [mag]	$V-I$	P [d]	dP/dt [d/yr]
18:01:57.16	-30:17:34.6	16.54	1.37	1.3642907	-4.900E-06
18:01:15.04	-29:50:50.7	17.74	1.63	1.7027067	-3.700E-06
18:03:59.26	-29:59:41.2	16.07	1.11	1.2046764	-2.300E-06
18:02:44.75	-30:19:51.9	15.85	1.26	1.0911776	-2.100E-06
18:02:44.24	-29:48:45.4	15.55	1.16	0.8556117	-1.700E-06
18:03:53.87	-30:19:19.8	16.75	1.26	0.8084745	-1.600E-06
18:01:52.74	-30:18:17.9	16.85	1.37	1.0291539	-1.400E-06
18:02:24.11	-30:07:38.7	17.10	1.42	0.8101012	-1.300E-06
18:01:59.16	-29:45:34.4	15.98	1.28	0.8924708	-8.300E-07
18:02:37.56	-30:20:17.7	17.38	1.33	0.8552266	-8.100E-07
18:03:21.07	-29:59:32.3	16.41	1.12	0.9480481	-7.300E-07
18:03:56.25	-29:49:46.0	16.61	1.33	0.8890325	-4.600E-07
18:02:13.56	-29:48:37.8	16.70	1.30	0.9320552	-4.000E-07
18:01:50.77	-29:52:46.0	18.05	1.20	0.8133902	-3.100E-07

evolutionary state of the system. The present work aims to explore the current prospects of searching for similar systems and stellar merger candidates as a whole.

The AAVSO VSX database was used to select periodic variables classified as contact binaries. Of the systems in the 1.1 – 1.8 d period range 207 were identified in the SDSS catalog. By utilizing the color-temperature relations derived by Boyajian et al. (2013) approximate surface temperatures for 128 systems were obtained. In 15 cases the calculated temperatures are in the 4200 – 4800 K range and the maximum possible reddening is lower than 0.07 mag. If correctly classified as W UMa-type variables, these 15 systems may have similar parameters as the V1309 Sco progenitor. Therefore, a more detailed exploration of these systems could bring an insight into the physics of a red nova progenitor.

An prediction of a stellar merger in the near future would require evidence that the orbital period is decreasing. A steady decrease of the orbital period results in a parabolic ETV curve with a negative second derivative. The 31 Kepler systems with parabolic ETV curves selected by Conroy et al. (2014) were visually classified. Two of them were selected as potential stellar merger candidates and require further observations. A search among the fainter OGLE contact binaries yielded 14 systems with $P > 0.8$ d and a steady period decrease.

The number of known eclipsing binaries is still insufficient to select exact twins of the V1309 Sco progenitor. However, it is already sufficient to select systems with similar parameters and, possibly, in a similar evolutionary state. Some of those also have apparent magnitudes comparable to the V1309 Sco progenitor (Tab. 2). Upcoming missions such as GAIA and LSST are expected to discover millions of eclipsing binaries (e.g. Prša et al. 2011). Therefore the number of known contact binaries with evolved components may increase by a factor of $\sim 10^2$ in the following decade.

References

- [1] Ahn C. P., Alexandroff R., Allende Prieto C. et al., 2012, *ApJS*, 203, 21
- [2] Bond H. E., Henden A., Levay Z. G. et al., 2003, *Nature*, 422, 405-408
- [3] Boyajian T. S., von Braun K., van Belle G. et al., 2013, *ApJ*, 771, 40
- [4] Conroy K. E., Prša A., Stassun K. G. et al., 2014, *AJ*, 147, 45
- [5] Drake A. J., Graham M. J., Djorgovski S. G. et al., 2014, *ApJS*, 213, 9
- [6] Kamiński T., Menten K. M., Tyłenda R. et al., 2015, *Nature*, 520, 322-324
- [7] Kochanek C. S., Adams S. M. and Belczynski K., 2014, *MNRAS*, 443, 1319-1328
- [8] Kubiak M., Udalski A. and Szymanski M. K., 2006, *AcA*, 56, 253
- [9] Kulkarni S. R., Ofek E. O., Rau A. et al., 2007, *Nature*, 447, 458-460
- [10] Kurtenkov A. A., Peshev P., Tomov T. et al., 2015, *A&A*, 578, L10
- [11] Mason E., Diaz M., Williams R. E., Preston G. and Bensby T., 2010, *A&A*, 516, A108
- [12] Molnar L. A., Van Noord D. M., Steenwyk S. D., Spedden C. J. and Kinemuchi K., 2010, *AAS Meeting Abstracts*, 225, 415.05
- [13] Prša A., Pepper J. and Stassun K. G., 2011, *AJ*, 142, 52
- [14] Rich R. M., Mould J., Picard A., Frogel J. A. and Davies R., 1989, *ApJ*, 341, L51-L54
- [15] Slawson R. W., Prša A., Welsh W. F. et al., 2011, *AJ*, 142, 160
- [16] Tyłenda R., Hajduk M., Kamiński et al., 2011, *A&A*, 528, A114
- [17] Tyłenda R. and Soker N., 2006, *A&A*, 451, 223-236

Table 5. Photospheric temperatures of 128 contact binaries with periods in the 1.1 – 1.8 d range and galactic latitudes $|b| > 20^\circ$.

α (J2000.0)	δ (J2000.0)	P [d]	Mag.	Amp.	T_{eff} [K]	σ_T [K]	α (J2000.0)	δ (J2000.0)	P [d]	Mag.	Amp.	T_{eff} [K]	σ_T [K]
00:24:35.21	07:34:25.5	1.7100	13.92	0.08	3306	132	13:02:13.45	34:05:07.2	1.6378	16.57	0.34	5801	61
00:34:56.35	24:15:04.9	1.5581	17.21	0.28	6310	93	13:03:46.26	00:46:43.2	1.3072	16.68	0.66	5023	81
00:44:12.88	20:11:07.8	1.7533	13.75	0.06	4750	77	13:06:00.14	18:00:46.7	1.3074	16.68	0.14	4315	70
00:49:18.55	39:52:29.7	1.1784	15.93	0.36	6354	39	13:24:23.64	07:58:59.8	1.6895	16.91	0.19	6561	118
00:58:44.79	18:43:29.7	1.2727	17.38	0.23	4103	42	14:07:20.29	-12:45:15.9	1.4548	15.10	0.35	6563	81
01:02:35.85	40:27:47.4	1.5630	17.70	0.46	5233	53	14:18:14.46	41:36:41.8	1.3134	16.09	0.22	6236	51
01:04:25.72	-05:03:30.3	1.2006	15.04	0.18	3891	18	14:21:14.77	35:28:38.9	1.5851	16.14	0.09	4592	26
01:56:09.97	28:40:18.7	1.2016	14.22	0.12	7415	81	14:25:27.50	30:41:49.9	1.1985	17.91	0.41	3539	71
02:09:03.05	-04:26:14.7	1.5781	18.17	0.31	4496	116	14:27:59.50	06:54:24.0	1.7529	15.50	0.09	4937	48
02:23:29.59	11:57:23.6	1.2330	14.66	0.17	4864	100	15:02:20.15	26:21:12.1	1.7954	15.94	0.18	4729	83
02:31:59.75	-03:58:32.3	1.4094	14.62	0.11	3373	100	15:13:48.47	12:32:11.0	1.5098	16.69	0.10	5093	61
02:48:49.65	19:10:16.0	1.6974	14.34	0.18	5721	130	15:20:53.17	-13:23:15.7	1.7053	14.78	0.19	5987	147
02:56:11.59	32:42:52.4	1.2569	13.40	0.28	5340	55	15:35:10.57	01:21:19.1	1.5204	16.13	0.69	5369	109
03:04:26.92	18:36:33.2	1.3890	17.39	0.44	6385	134	15:35:46.16	17:36:01.8	1.3456	13.97	0.08	5453	98
03:18:05.55	17:55:27.0	1.1015	14.78	0.09	5591	54	15:36:08.42	21:09:38.2	1.5163	18.22	0.46	6402	34
03:23:29.17	-00:34:49.3	1.7183	15.66	0.15	5152	76	15:39:45.08	07:20:46.2	1.3350	16.21	0.26	6802	73
03:54:59.63	01:16:16.3	1.5202	15.89	0.32	3631	111	15:50:21.58	12:22:16.2	1.1158	17.48	0.50	6583	94
04:28:43.41	-06:53:22.3	1.3491	13.99	0.15	3618	140	15:51:53.35	04:15:29.8	1.4075	14.36	0.14	6060	85
04:45:50.71	11:34:57.2	1.3164	15.29	0.35	4723	110	16:06:30.09	33:13:44.1	1.5736	14.81	0.11	6257	64
04:52:13.32	00:56:18.4	1.6971	14.68	0.09	6638	33	16:15:39.64	12:47:23.2	1.1409	16.15	0.24	5104	101
04:56:06.10	-01:07:53.1	1.1575	14.56	0.18	3672	62	16:20:45.25	34:57:41.6	1.2987	16.98	0.13	6468	63
05:06:27.90	-00:21:30.0	1.2615	15.59	0.10	3382	22	16:26:09.66	05:13:20.5	1.4847	15.89	0.13	4102	44
05:27:06.19	-05:58:27.6	1.4527	15.74	0.11	3283	58	16:29:45.49	-02:11:41.6	1.5380	17.38	0.33	5377	97
07:26:18.08	31:55:03.0	1.1579	15.71	0.22	4744	67	16:30:29.76	20:23:16.4	1.6452	17.40	0.42	6001	139
07:34:32.94	36:48:28.5	1.1646	17.38	0.31	4519	96	16:30:42.51	53:12:58.7	1.1418	17.59	0.34	5588	69
07:38:45.77	34:57:20.3	1.5792	13.30	0.17	5481	93	16:41:42.79	20:20:37.2	1.1087	15.14	0.10	6123	60
07:39:47.77	32:40:24.6	1.5975	13.31	0.14	5390	32	16:52:47.42	16:18:35.1	1.6941	13.84	0.19	4130	75
08:05:06.44	14:51:38.3	1.3981	17.58	0.26	6126	41	16:56:09.74	42:42:19.7	1.2699	15.52	0.18	4383	127
08:05:43.15	40:46:38.5	1.5851	15.40	0.08	4908	37	17:00:41.65	12:05:31.6	1.5080	14.65	0.11	6036	83
08:11:08.14	30:38:03.3	1.6462	14.48	0.06	4105	92	17:10:08.19	32:56:11.3	1.2843	17.80	0.36	5398	56
08:17:46.29	13:05:05.7	1.5947	14.90	0.08	4519	64	17:12:06.21	40:55:37.8	1.5102	15.77	0.16	5504	60
08:19:42.20	41:29:47.9	1.6497	16.13	0.14	3743	74	17:14:28.01	10:13:10.7	1.7623	15.92	0.14	4479	61
08:22:08.52	09:07:27.1	1.2965	17.93	0.31	6077	82	17:18:55.47	62:03:28.6	1.1993	14.15	0.40	6800	28
08:29:50.38	23:06:51.8	1.6032	16.07	0.10	6935	32	17:20:10.09	08:26:36.7	1.6102	15.41	0.42	5945	121
08:31:48.57	29:44:44.0	1.4136	14.93	0.12	4445	89	17:25:53.14	61:17:15.6	1.1309	14.41	0.27	7551	9
08:43:34.88	03:09:57.0	1.3806	16.47	0.10	3970	13	17:27:21.85	27:50:55.3	1.5273	18.01	0.44	5283	45
08:45:36.01	20:13:00.6	1.3800	17.00	0.11	6297	88	17:35:10.22	20:31:02.2	1.2142	16.37	0.18	5645	75
08:49:23.10	10:51:29.1	1.1003	16.43	0.10	4148	24	17:45:56.93	42:24:00.5	1.2803	16.52	0.10	6162	81
08:58:13.10	13:38:20.5	1.4357	14.95	0.12	4886	101	20:53:56.62	-01:09:43.6	1.6379	14.14	0.17	5021	65
09:01:32.24	01:01:01.8	1.5418	16.27	0.10	6112	83	21:00:34.55	-11:38:46.2	1.1281	17.91	0.45	6798	148
09:03:58.49	16:17:12.7	1.2009	16.72	0.17	5154	80	21:15:59.21	-10:50:10.4	1.3021	14.64	0.13	6256	77
09:05:04.20	23:44:07.1	1.3327	16.13	0.91	6396	85	21:48:28.60	09:03:36.5	1.4246	16.87	0.17	5994	131
09:06:32.35	11:29:30.8	1.1806	15.83	0.13	4995	86	21:48:47.47	-05:48:26.1	1.5972	17.57	0.22	6200	90
09:07:14.17	13:27:20.7	1.1835	16.97	0.36	7224	51	21:50:41.97	12:37:08.2	1.2976	15.94	0.09	4000	27
09:15:04.25	29:52:40.1	1.3513	14.39	0.28	5288	18	21:58:23.25	07:18:31.5	1.2970	16.52	0.11	6116	75
09:46:14.73	16:47:06.0	1.6007	15.31	0.25	4750	100	22:00:17.17	23:21:32.0	1.6262	15.04	0.43	4948	48
09:46:56.35	40:14:59.8	1.4679	14.67	0.23	5378	84	22:07:38.21	30:03:53.1	1.1424	14.65	0.37	5292	73
09:50:00.13	23:49:52.2	1.1698	15.44	0.09	3970	21	22:16:20.77	07:33:57.2	1.1351	15.60	0.07	4026	15
09:54:04.15	05:56:33.0	1.3438	16.05	0.12	3796	35	22:29:09.15	17:37:23.4	1.3664	14.60	0.08	4568	46
10:00:01.70	24:23:05.1	1.2955	15.85	0.15	4213	48	22:32:25.40	06:00:48.3	1.4293	16.12	0.11	5879	104
10:02:30.35	50:18:08.8	1.2404	15.51	0.23	4760	74	22:33:22.32	30:33:25.0	1.2756	15.90	0.24	5848	105
10:38:20.36	12:46:14.9	1.3373	15.72	0.16	3267	84	22:42:01.99	-05:25:00.1	1.7298	16.58	0.48	5144	75
10:38:44.77	13:45:51.1	1.3263	14.63	0.10	3456	94	22:42:18.68	14:24:09.1	1.4598	16.37	0.11	3452	64
10:49:39.27	33:45:22.1	1.3964	14.55	0.41	5217	52	22:43:42.38	26:02:16.9	1.1415	15.13	0.19	6710	16
11:00:13.96	36:04:29.0	1.6927	16.30	0.32	6793	14	22:45:43.47	07:47:14.2	1.3456	15.68	0.09	5147	93
11:07:43.59	21:13:51.7	1.2885	17.67	0.24	6167	40	22:56:43.91	-02:56:22.3	1.1710	15.51	0.10	3533	54
11:08:58.93	31:45:52.3	1.2302	16.07	0.37	5625	106	23:08:23.17	15:17:11.5	1.5196	17.39	0.37	4804	80
11:11:01.12	03:31:00.9	1.5349	14.49	0.41	6009	75	23:12:46.22	17:13:14.5	1.1487	14.92	0.37	6403	56
11:16:12.89	00:17:52.6	1.4245	16.13	0.51	5017	71	23:15:47.32	12:29:37.5	1.7325	15.28	0.19	4679	75
11:18:17.29	-00:14:45.2	1.4907	15.95	0.75	5875	54	23:22:22.15	22:06:22.3	1.6478	17.02	0.16	5218	42
12:10:22.21	35:46:55.4	1.5242	17.86	0.19	6231	104	23:33:31.70	14:37:43.1	1.1161	17.37	0.70	4884	75
12:30:23.09	-02:23:36.7	1.3086	16.38	0.11	6382	91	23:36:48.71	35:10:36.9	1.1653	14.53	0.15	3987	26
12:32:25.24	04:02:34.8	1.3214	16.43	0.15	6277	54	23:54:34.83	35:28:09.3	1.7990	14.41	0.16	5706	121
12:48:15.08	13:14:21.4	1.2449	17.75	0.27	6171	78	23:55:46.62	29:36:20.6	1.1607	15.91	0.57	5120	89